Magnetoelectric sensors: A review

Junqi Gao ^{1,2,3}, Bing Li^{1,2,3}, Qingwei Liu ^{1,2,3}, Ying Shen ^{1,2,3*}, Zhaoqiang Chu ^{1,2,3}, Jianglei Chang ⁴, Shuxiang Dong⁴, Zhongqiang Hu⁵, Ming Liu⁵

¹ National Key Laboratory of Underwater Acoustic Technology, Harbin Engineering University, Harbin 150001, China
² Key Laboratory of Marine Information Acquisition and Security (Harbin Engineering University), Ministry of Industry and Information Technology, Harbin 150001, China

College of Underwater Acoustic Engineering, Harbin Engineering University, Harbin 150001, China
 Institute for Advanced Study, Shenzhen University, Shenzhen 518060, China
 School of Electronic Science and Engineering, Xi'an Jiaotong University, Xi'an 710049, China

Multiferroic materials possess at least two fundamental properties of ferroelectricity, ferromagnetism, and ferroelasticity. This advanced coupling effect between different properties endows multiferroic materials with new characteristics. As a result, these materials have high potential for applications in various fields. One characteristic that the magnetoelectric (ME) coupling effect can achieve is electric-field-controlled magnetization or magnetic-field-controlled polarization. This effect opens a new direction for the development of low-power and small-sized electronic devices. This review first provides a brief introduction of the development history and recent studies of ME materials. We then introduce the latest research progress on ME sensors and summarize their engineering applications in magnetic detection. Finally, we conclude by addressing potential future work on ME effect enhancement and potential engineering applications.

Index Terms—Magnetoelectric materials, Composites, MEMS, Magnetic field sensor

I. INTRODUCTION

Magnetic detection technology holds significant research value in detecting ferromagnetic materials, which are prolifically used today. The primary method for detecting magnetic fields involves the interaction and connection between magnetic and electric phenomena. These have led to the development of various magnetic sensors, such as optically pumped sensors, fluxgate sensors, magnetoresistive sensors, and Hall sensors. In the latter half of the twentieth century, magnetoelectric (ME)-coupled materials attracted significant interest because of their exceptional performance in terms of the ME coupling coefficient $\alpha_{\rm ME}$. This indispensable parameter determines the ME conversion ability and holds immense research value in magnetic field detection technology [1].

As a coupling effect, the ME effect connects two physical fields. Thus, it has potential for investigating and identifying magnetic and electric fields [2]. Over the last 63 years, researchers have carried out extensive studies on ME materials and their effects. Representative materials include single-phase ME materials [3-5], complex-phase granular ME composites [6], and complex-phase laminated ME-coupled materials [7, 8] (complex-phase bulk ME composites and complex-phase thin-layer ME composites), among others. Fig 1 illustrates the ME effect and crucial stages in development of materials [9].

ME effects can be classified into direct ME coupling and reverse ME coupling. Direct ME coupling means that the magnetic field triggers the electric polarization effect. Reverse

This work was supported in part by the National Key R&D Program of China (Grant No. 2022YFB3205700), in part by National Natural Science Foundation Youth Program (Grant No. 62101151), and in part by the Natural Science Foundation of Heilongjiang Province (Grant No. YQ2021F001), in part by Central Universities Basic Research Operating Costs Project (Grant No. 3072024XX2604). Corresponding author: Ying Shen (e-mail: shenying@hrbeu.edu.cn).

ME coupling means that the electric field prompts the magnetization effect[10]. Compared with other magnetic field sensors, direct ME coupling effect sensors are more cost effective, less noisy, less energy intensive and more sensitive. Thus, they are ideal for magnetic field detection [11]. The latest research has shown that ME sensors have been successfully applied in various fields, including target detection, non-destructive testing, speed and angle sensing, current sensing, magnetic field energy harvesting, low frequency communication and biomedical magnetic field detection [12-16].

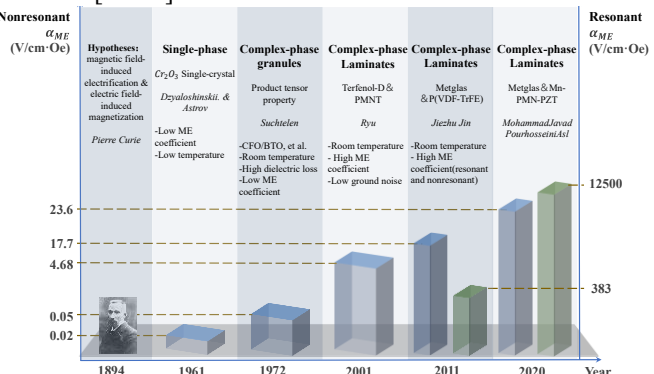


Fig 1 Important developmental nodes in ME effects and materials research.

II. ME MATERIALS AND STRUCTURES

Pierre Curie first suggested the concept of ME intrinsic effects in 1894 [17]. In 1926, the phenomenon of ME coupling was named the "ME effect" by Peter Debye [18]. In 1961, V. J. Folen et al. observed the ME effect in a single Cr₂O₃ crystal [19]. The ME effect has subsequently been observed in many single-phase materials that exhibit magnetoelectricity. Various material systems have the potential to exhibit ME effects, such as Fe₂TeO₆, DyFeO₃, FeCrWO₆, FeSb₂O₄, V₂WO₆, Cr₂WO₆, Ca₂FeAlO₅, Eu₃O₄, and β-FeNaO₂ [20]. However, single-

phase ME materials have never been widely recognized or used because of their weak ME effect and because they can operate only at very low temperatures [21]. It was not until the 1970s, when van Suchtelen introduced the concept of multiphase ME composites [20], that the ME effect was reemphasized. The discovery of ME composite materials exhibiting high ME coefficients holds enormous potential for future applications, thereby attracting significant attention and becoming a popular research topic in research. In 1972, Suchtelen proposed the concept of complex-phase materials and summarized the coupling effects between different physical and chemical effects [20]. At the same time, Boomgaard et al. [22] utilized ceramic-based ME-composite materials with piez0electric and magnetostrictive effects, resulting in ME effects. The emergence of complex-phase materials has opened the era of ME-coupled materials working at room temperature. Thus, their application prospects have been greatly improved. However, owing to the rough compositing method, the ME conversion efficiency of these types of polyphase materials is low.

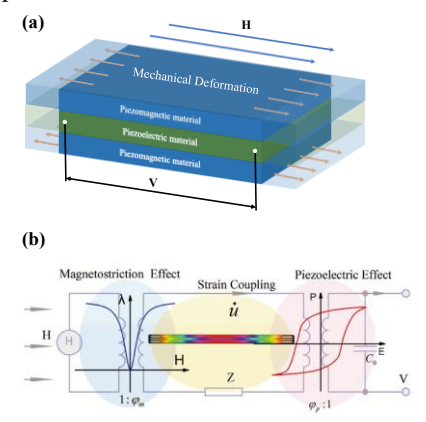


Fig 2 (a) ME structure and coupling principle. (b) Schematic diagram of the principle of the ME effect (equivalent circuit diagram method) [9].

In 2001, Ryu et al. improved the composite mode and achieved innovative results [23]. A great breakthrough has been made in magneto-electrically coupled composites by making a sandwich structure of piezoelectric and

magnetostrictive layers. It have much higher ME coefficients than those of previous ceramic-based composite and single-phase ME materials. The structure of the magneto-electrically coupled material as well as the coupling mechanism can be explained via the (a) a conceptual diagram and (b) the equivalent circuit diagram approach, as shown in Fig 2. In this case, the magneto-mechano-electric coupling relationship is shown in Eq. (1).

$$ME \, effect = \frac{V}{H}$$

$$= \frac{electric}{mechanical} \times \frac{mechanical}{magnetic}$$
 (1)

This investigation has attracted lots of interests in the research of ME coupling effect. Layered composite ME materials also utilize the product effect mentioned above to achieve ME coupling on the basis of magnetostriction and piezoelectric effects. When an external magnetic field is applied, the magnetostrictive phase produces a certain deformation. It is transferred to the piezoelectric material by stress transfer. On the basis of the piezoelectric effect, induced charges are generated at both poles. Currently, there are many types of layered composite ME materials in terms of composite structure and material composition. Piezoelectric materials include (1-x) [Pb (Mg_{1/3}Nb_{2/3})O₃]-x[PbTiO₃] (PMN-PT) single crystals, Pb (Zr,Ti)O₃ (PZT) ceramics, (CH₂CF₂)_n (PVDF), BaTiO₃ lead-free piezoelectric ceramics, etc. Magnetostrictive materials include Fe-Ga single crystals, Fe-Ni alloys, CoFe₂O₄, Terfenol-D single crystals, amorphous alloy Metglas, etc. There are also various ways to connect layers, including hot-pressed epoxy resin bonding, conductive silver adhesive bonding, electroplating, etc.

To improve the performance of ME laminated coupled materials, optimizing the coupling structure and mode of operation has been the focus of research for many years. **Table 1** illustrates the characteristics and properties of the more typical laminated ME-coupled materials from 2001 to the present.

Table 1 Structures and Properties of Various ME Composites Table

Table 1 Structures and 1 Toperties of Various ME Composites Table						
Composition	Year	Connectivity	Working Mode	Working Temperature	Nonresonance α_{ME} (V/cm·Oe)	Resonance $\alpha_{ME}(V/cm\cdot Oe)$
NiFe ₂ O ₄ /PZT[24]	2001	2-2	L-T	Room Temperature	1.5	/
Terfenol-D/PZT[7]	2002	2-2	L-T	Room Temperature	5	/
Metglas/PVDF[25]	2006	2-2	L-T	Room Temperature	7.2	310
Metglas /PZT[26]	2006	2-1	L-L	Room Temperature	22	500
Terfenol-D/PZT[27]	2007	3-1	L-L	Room Temperature	1	18
Metglas/P(VDF-TrFE)[28]	2011	2-2	L-L	Room Temperature	17.7	383
Metglas/PMN-PT[29]	2011	2-1	L-L	Room Temperature	45	1100

Lanthanum gallium tantalite/permendur[30]	2012	2-2	/	Ultra-high temperature (>1000°C)	2.3	720
FeCoSiB/(Pt)/AlN in vacuum[31]	2013	2-2	L-T	Room Temperature	/	20000
FeCoSiB/(Pt)/AlN[32]	2016	2-2	L-T	Room Temperature	/	5000
Metglas/PMN-PT without laser treatment[9]	2017	1-1	L-T	Room Temperature	29.3	5500
Metglas/PMN-PT with laser treatment[9]	2017	1-1	L-T	Room Temperature	22.9	7000
Metglas/LiNbO ₃ [33]	2018	2-2	L-T	Room Temperature	1.9	1704
Metglas/Mn-PMN-PZT with laser treatment[34]	2020	1-1	L-T	Room Temperature	23.6	12,500

In the past two decades, the research of layered ME composites has mainly focused on bulk ME composites. In recent years, the development of bulk ME composites tends to be mature. Fig 3 visualizes the development of the properties of bulk ME composites. Moreover, to further expand the application potential of ME-coupled materials, researchers are gradually favouring the study of smaller thin-film ME composites. Miniaturized materials can be applied to a variety of precision instruments to achieve more functions. In addition, the development of piezomagnetic and piezoelectric materials is maturing. This allows ME composites to exhibit consistently excellent performance at room temperature. However, the current literature shows that the study of the adaptability of this type of material at different temperatures still needs to be improved.

The development of ME-coupled materials has enabled a growing number of materials to achieve high ME conversion factor performance at room temperature. Furthermore, the advances made by researchers in this field have attracted significant interest because of the emergence of resonance enhancement properties. The ME conversion coefficient (MCC), a key performance parameter, is affected by material selection and structural changes. It also varies with the DC bias applied at both ends of the material. Each composite has a different optimal bias magnetic field size. Moreover, the ME conversion coefficient of each composite is different. Notably, the ME conversion effect generated by the material is not affected by positive and reverse coupling. The ME conversion coefficients of various ME composites at room temperature and optimal bias conditions are compared below [35].

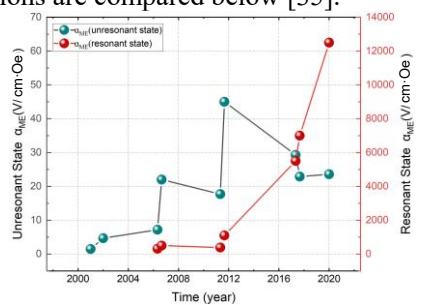


Fig 3 Development of ME coefficients in the resonant and nonresonant states

of bulk ME composites since 2001.

III. ME MAGNETIC SENSORS

Since the concept of multiplicative properties of complex-phase ME materials was introduced [20], there has been a surge in academic research on complex-phase materials. Compared with single-phase materials, complex-phase materials avoid the difficulty of unifying the electrical and magnetic order within a single material [36]. In the 1970s, the eutectic method of preparing particulate complex-phase ME materials became the mainstream method of research and development. However, the material obtained via this method has more pores between the particles of the two phases of the material. This results in a low stress-transfer efficiency and low ME coefficient [6]. Therefore, the academic enthusiasm for complex-phase ME materials has gradually declined.

In 2001, Ryu et al. published their latest results on ME materials [23]. They prepared laminated sandwich composite ME materials by using a Terfenol-D piezomagnetic material and a PZT single-crystal piezoelectric material. The ME coefficient of the composite material obtained via this method is as high as 4.68 V/cm·Oe. Compared with previous complex-phase ME materials, it achieves a 36-fold enhancement. In addition, this material can work at room temperature, which means that it has very high potential for application. Since then, there has been a surge of research in the academic community about layered ME composites.

Laminated composite ME materials work on the principle of ME conversion on the basis of the performance multiplier effect, using the magnetostrictive effect and the piezoelectric effect to realize the ME coupling effect. When a magnetic field is applied to a composite material, the shape of the piezomagnetic material changes through its magnetostrictive properties. The connection of the two phases transmits the strain to the piezoelectric phase and produces an electrical output. Many studies and attempts have been made to achieve efficient conversion between magnetoelectric materials and to develop new ME sensors. The key factors determining the efficiency of ME

conversion are mainly classified as follows: a. the material properties of the phases composing the composite (piezomagnetic coefficient, piezoelectric coefficient, permeability, coefficient of elasticity, dielectric constant, etc.) [28, 37-40], b. The morphology of the two phases (2-2, 2-1, 1-1) and the mode of operation (according to the direction of polarization and magnetization: L-L, L-T, T-T, T-L) [41, 42], c. the thickness/volume ratio of each phase [43-46], and d. composite preparation techniques [28, 47]. Considering the practical application requirements of the sensors, the DC bias magnetic field, operating frequency and noise floor level of the material are also important. At the beginning of the 21st century, research on the above factors was very popular. On the basis of these factors, several of the most representative ME sensors are introduced below.

A. Bulk Sensors

Among ME sensors, bulk sensors are the most developed. This type of sensor is strongly influenced by the material morphology. On this basis, they can be divided into three categories: (2-2), (2-1) and (1-1). These three categories of bulk sensors are described below.

1) (2-2) composite mode:

The (2-2) composite mode was discovered in 2001. The

most representative of the (2-2) composite mode is the Terfenol-D/PZT sandwich-structured ME composite mentioned above. In the same year, with reference to this material, a kind of ME composite material composed of NiFe₂O₄/PZT was subsequently proposed. However, the ME coupling coefficient of this material was only 1.5 V/cm·Oe. Thus, the performance of a piezomagnetic material directly affects the performance of the ME composite material.

In 2003, Dong et al. developed a sandwich laminate structure called L-L [48]. It consists of two Terfenol-D layers magnetized in the lengthwise direction (or longitudinal direction) and two hard PZT piezoelectric ceramic layers also polarized in the longitudinal direction. As shown in Fig 4(a), two PZTs with opposite polarization directions were arranged as a monolayer between the Terfenol-D materials. The long shape of the structure enhanced the main vibration along the longitudinal axis. A significant enhancement of the ME effect was found near the resonance, with a maximum induced ME voltage of 10 V/Oe at resonance. Subsequently, Dong et al. proposed L-T, T-L, and T-T operating modes. They applied the equivalent circuit methodology to theoretically model the four different modes of operation of the ME composites [49]. The ME coupling coefficient at the resonant frequency becomes the key performance index of ME composites.

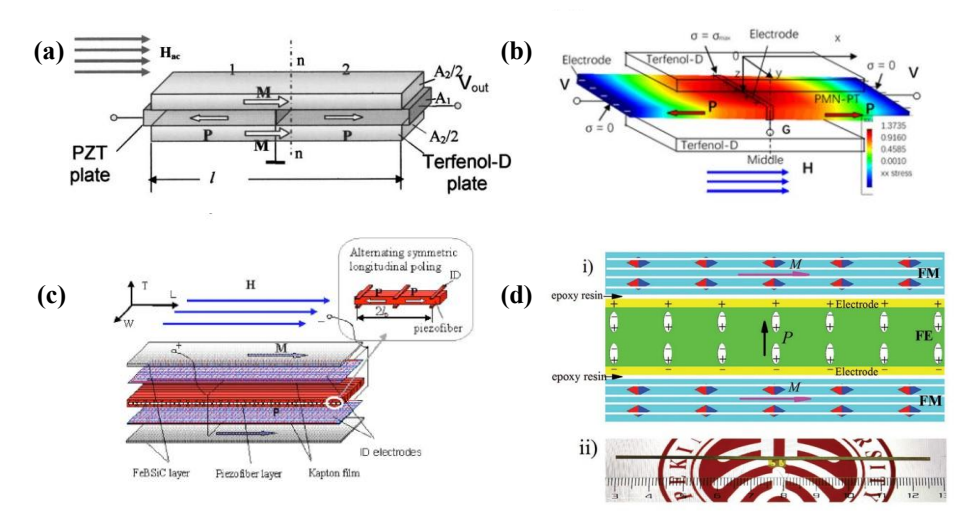


Fig 4 (a) Configuration of an L-L mode magnetostrictive/piezoelectric laminate composite[48]. (b) Push-pull ME laminate[50]. (c) Multi push-pull L-L ME structure configuration[26]. (d) A (1-1) laminated ME composite[9].

In the following years, the study of the different composite modes and the related principles of the operating modes became a popular research topic. Dong's research group experimentally verified the performance differences among the two most common operating modes: L-T and T-T [41]. Similar to the modelling results, the performance of the L-T operating mode outperformed that of the T-T mode.

To further optimize the elastic coupling between the layers, an ME laminate composite with push-pull mode was developed on the basis of the L-L mode. Dong et al. improved a (2-2) composite L-L push-pull-structured ME-coupled material on the basis of the characteristics of the L-L operating mode. The material consists of symmetric longitudinally

polarized piezoelectric PbMg_{1/3}Nb_{2/3}O₃-PbTiO₃ crystals and two longitudinally magnetized magnetostrictive Tb_{1-x}Dy_xFe₂ layers, as shown in Fig 4(b). The polarized piezoelectric crystals operate in push–pull mode with a maximum stress concentration in the centre and both ends free. The composite obtained from this structure has a large ME voltage coefficient of 1.6 V/Oe at low frequencies, which can be increased to 20 V/Oe at the resonance drive [50]. The performance characteristics of this material are significantly better than those of the previous L-T operating mode composites. This opens a new path for the structural development of ME-coupled materials.

In 2006, the (2-2) composite L-T mode ME-coupled sensor

developed by J. Zhai and S. Dong et al. achieved an ME factor of 7.2 V/cm·Oe in the nonresonant state and 310 V/cm·Oe in the resonant state [25]. However, there is still much room for improvement relative to the theoretical performance.

In 2011, J. Jin et al. developed multiferroic polymers as alternative piezoelectric ceramics with excellent performance [28]. They further improved the ME coupling coefficients of the L-L mode under the (2-2) composite to 17.7 V/cm·Oe in the nonresonant state and 383 V/cm·Oe in the resonant state.

In the early stage of ME sensor material development, (2-2) bulk composites dominated the research, and various studies have demonstrated that the performance is still not ideal; thus, there is an urgent need to investigate other composite mode materials.

Notably, in recent years, (2-2) ME composites have been used to create special sensors through structural adjustments.

In 2018, Jitao Zhang et al. proposed a bidirectional tunable ferrite-piezoelectric trilayer ME inductors [51]. It consists of a symmetrical three-layer solenoid with gallium-doped nickelzinc ferrite and PZT. Its permeability changes under the action of applied magnetic field or electric field, resulting in bidirectional tuning of inductance L. The maximum tunability of this inductor can reach $\Delta\,L_{max}/L_{min}\approx 571\%$ under low magnetic field.

In addition, Mirza I. Bichurin et al. of Novgorod State University, investigated self-biased two-domain ME current sensors in 2020[52]. The ME gradient structure shown in Fig 5. The sensor has the characteristics of a noncontact ME current sensor, with a current range of up to 10 A and a sensitivity of 0.9 V/A, whereas the current consumption rate does not exceed 2.5 mA, with a linearity accuracy of 99.8%. The device operates in bend mode and does not require lead elements. It has the characteristics of simple operation, high sensitivity and low working frequency.

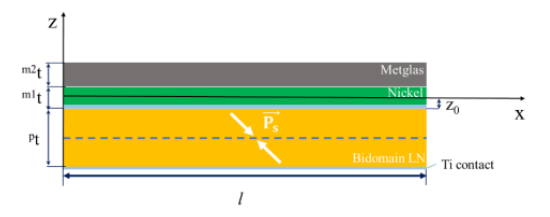


Fig 5 Schematic view of the ME gradient structure[52].

2) (2-1) composite mode:

The performance of L-L mode ME laminates was still far from the theoretical performance until 2006. Dong et al. reported ME laminate composites in a (2-1) connection configuration. This composite consists of a one-dimensional connected piezoelectric PZT fibre laminate and two highly magnetostrictive FeBSiC alloy Metglas layers [26]. As shown in Fig 4(c), multiple piezoelectric fibres form multiple push–pull modes, thus optimizing the stress transfer and increasing the dielectric capacity. The L-L modal laminate under this structure has a high ME coefficient of 20 V/cm·Oe at nonresonant frequencies, which is substantially enhanced to

500 V/cm·Oe at resonant frequencies. This achievement reveals an ME potential that is close to the ideal value and represents the opening of a new section in the research, development, and application of ME composites.

At the beginning of the twenty-first century, Metglas amorphous alloys and Terfenol-D single crystals presented excellent piezomagnetic coefficients and became the preferred magnetostrictive materials. In addition, the theoretical model shows that the material piezoelectric coefficient d₃₃ is the key to influencing the strength of the ME response [42]. The [011]-oriented PMN-PT crystals have excellent d₃₃ values and transverse piezoelectric properties and are thus widely used as piezoelectric phases [39, 53]. In addition to piezomagnetic and piezoelectric materials, laminated ME composites also contain an interfacial bonding layer and an electrode layer. The interfacial bonding layer, as a key medium for stress conduction, needs to be selected because of its low dielectric loss and high mechanical conduction efficiency. Since 2009, a research team at the University of Virginia, USA, has focused on optimizing the mechanical and dielectric properties of the interfacial bonding layer of laminated ME composites. It was found that reducing the thickness of the interfacial bonding layer reduces the dielectric loss. Therefore, the equivalent noise floor of the ME composites is attenuated. The dielectric loss coefficients of laminated ME composites using stycast epoxy resin are much lower [47].

As material selection and preparation techniques matured, the focus of research shifted to background noise reduction of and sensitivity enhancement. On this basis, much research has also been conducted at the University of Virginia in magneto-electrically coupled materials. In 2011, Y.J. Wang et al. improved and prepared a multiple push–pull structured ME-composite material using a Metglas magnetostrictive material and a PMNT single-crystal material, as shown in Fig 6(a-e). The structure uses flexible circuit board fork finger electrodes to achieve an ME coefficient of 52 V/cm·Oe in a quasistatic magnetic field. The output signal is passed through a charge amplification circuit to obtain a noise level of 5 pT/Hz^{1/2}@1 Hz [54]. The development of this material represents the ability of ME sensors to outperform well-developed fluxgates.

In the same year, Gao et al. proposed a differential (2-1) structure based on a PZT piezoelectric ceramic and Metglas magnetostrictive materials [55]. As shown in Fig 6(g), this structural design incorporates a piezoelectric layer consisting of two layers of polarized PZT fibres with double-sided electrodes in the middle. This can attenuate the external vibration noise of PZT fibre-based ME heterostructures. When employed in environments where there is vibration, the magnetic sensing capability of this structure outperforms that of traditional sensors. Sensors that use this differential structure decrease the external vibration noise approximately 10 to 20 dB at diverse frequencies when the ME voltage coefficient is also amplified. This approach creates novel possibilities for adapting ME sensors to their surroundings.

In 2015, Cong Fang et al. designed new multiple tandem L-T structured ME composites based on the L-T mode by

changing the polarization direction and connection method of the piezoelectric materials [56]. The material uses Metglas as the piezomagnetic phase and Mn-PMNT single crystals as the piezoelectric phase. Seven polarized single crystals are used for tandem connection. Thus, it can obtain a ME composite with the ME coefficient of 38.9 V/cm·Oe. Moreover, the material's dielectric loss is as low as 0.48%. And the noise level is only 0.87 pT/Hz^{1/2}@30 Hz. Owing to the extremely

low noise level, this structure has greater potential for practical applications.

Since then, the importance of material volume and the superiority of piezoelectric single-crystal materials have become apparent. Research has begun to move towards thinfilm ME sensors and piezoelectric single-crystal bulk ME sensors.

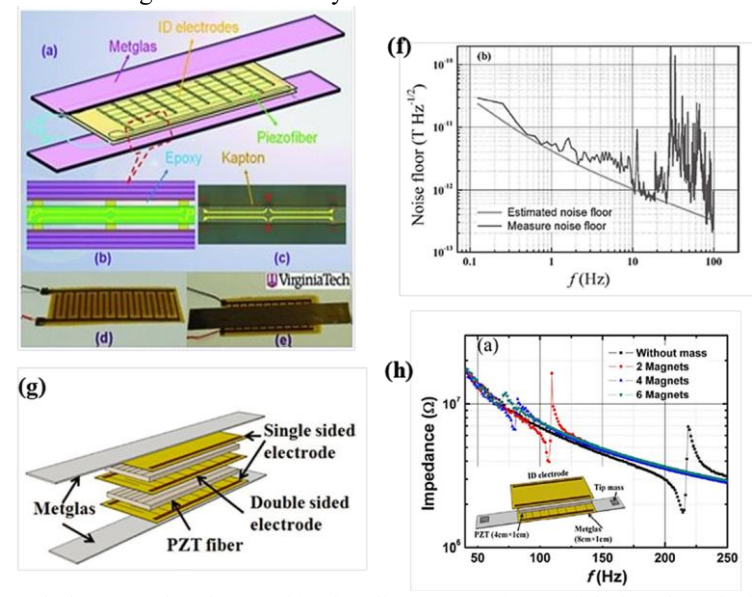


Fig 6 (a) Schematic structure of the Metglas/PMN-PT three-layer multipush—pull ME composite material. (b) Schematic diagram of the push—pull mode. (c) Optical microscopy image of a longitudinally poled push—pull element in the core composite. (d) Photo of the ID electrode/piezoelectric ceramic composite material. (e) Photograph of the Metglas/piezoelectric fibre composite ME sensor. (f) Noise floor of the Metglas/PMN-PT three-layer multipush—pull structured ME sensors. (a-f) ref [54]. (g) Schematic diagram of the differential structure low-noise ME sensor [55]. (h) Schematic structure of a bending mode ME sensor with magnets clamped at both ends and the impedance of the composite material for different numbers of clamped magnets [16].

3) 1-1) composite mode:

Chu et al. subsequently carried out a study on the (1-1)L-T mode. They developed [011]-oriented one-dimensional connectivity ME composites using a single PMN-PT single-crystal fibre as the piezoelectric phase and a laser-treated Metglas layer as the piezomagnetic phase, as shown in Fig 4(d). The material exhibits an ME coupling coefficient of 7000 V/cm·Oe in the resonant state, nearly seven times higher than the previous best value, and allows direct detection of a magnetic field of 1.35×10^{-13} T at room temperature [9].

B. Flexible Sensors

In 2021, a journal article on highly flexible sensors led by Nana Yang from Nanjing University of Science and Technology was published in APL Materials [57]. This article describes a cost-effective, flexible, and highly sensitive heterostructure ME sensor. It consists of a piezoelectric PZT thick film and Metglas foil, as shown in Fig 7. The sensor exhibited a powerful ME coefficient of 19.3 V/cm·Oe at low frequencies and 280.5 V/cm·Oe at resonant frequencies, as well as excellent mechanical durability.

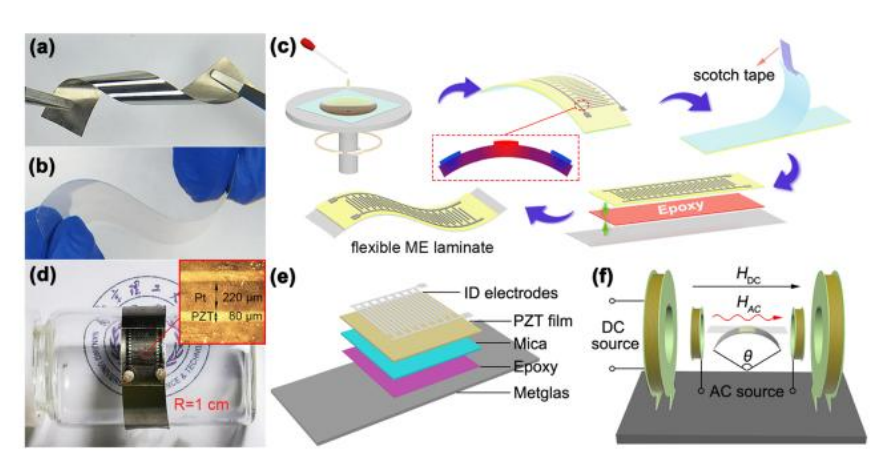


Fig 7 Photographs of flexible [57] (a) Metglas foil and (b) laminated structured mica substrate. (c) Schematic of the manufacturing process of flexible ME

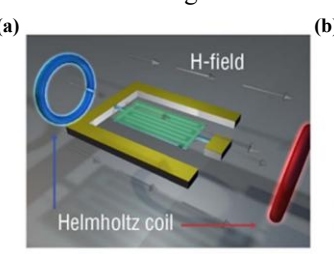
laminates. (d) Photograph of a flexible ME laminate affixed to a glass vial with a radius of 1 cm. The inset is an optical micrograph of the Pt IDE. (e) Schematic of the configuration of a flexible multipush–pull mode ME laminate. (f) Schematic diagram of an automated system for flexible ME characterization in the laboratory

C. MEMS Sensors

Unlike block ME sensors, microelectromechanical systems (MEMS) manufacturing techniques produce ME sensors that are more miniaturized. In recent years, owing to the continuous advancement of thin-film technology, research on the heterostructure of thin-film MEs has undergone rapid development [58]. For example, Greve et al. developed a thin-film MEMS composite composed of AlN and amorphous Fe₉₀Co₇₈Si₁₂B₁₀ [59]. AlN is different from amorphous soft magnetic alloy materials, has high piezomagnetic properties, and can be compatible with MEMS technology [32]. A great deal of research has been done on this type of material at the University of Kiel [32, 60-62].

Researchers have optimized a nanoelectromechanical system (NEMS) based on a MEMS. In recent years, owing to its miniaturization characteristics, this NEMS has been widely used in many fields.

The Sun research group at North-eastern University used ME NEMS thin films as ME resonators [62]. They designed a novel ME NEMS resonator based on an AlN/(FeGaB/Al₂O₃) × 10 ME heterostructure for detecting DC magnetic fields. It has an electromechanical resonance frequency of 215 MHz, at which the resonator is very sensitive to DC magnetic fields. This provides a new detection mechanism for ultrasensitive self-biased RF NEMS ME sensors. The structure of this resonator is shown in Fig 8, which consists of three material layers (from bottom to top): the differential electrode, an AlN film, and a FeGaB/Al₂O₃ film. When working, a DC magnetic field is applied in the longitudinal direction. The detection limit of the DC magnetic field can reach approximately 300 pT without shielding.



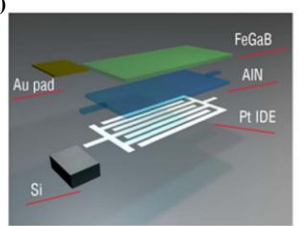


Fig 8 (a) Schematic of the NEMS magnetic field sensor. (b) Schematic of the layered structure of the NEMS magnetic field sensor [62].

In addition to detecting DC magnetic field strength, MEMS have also been developed for use in magnetic surface acoustic wave (MSAW) resonators for magnetic field sensing. Recently, a team of researchers at the University of Electronic Science and Technology of China (UESC) led by Huang Fei developed an MSAW resonator. It is composed of an AlN thin film, a Si layer and a magnetostrictive multilayer ((Fe₉₀Co₁₀)₇₈Si₁₂B₁₀-Cr) [63]. On the AlN layer, a set of IDTs composed of Ti/Au is used to excite Rayleigh waves, and the material specific thickness allows the sound energy to be coupled into the material. The resonator exhibits a sensitivity of up to 11 kHz/Oe along its hard axis. At the maximum magnetic sensitivity, the mass factor can reach approximately

3700. Because this resonator can also couple sound energy, it can meet the needs of wireless inquiry and high sensitivity at the same time. This discovery has clear potential in enabling wireless magnetic field sensors with miniaturization, low power consumption and high complementary metal oxide semiconductor (CMOS) compatibility.

IV. APPLICATIONS OF ME SENSORS

With the rapid development of ME sensors, scientific applications have also become popular. ME sensors based on the ME effect have been widely used in several different fields. **Table 2** summarizes the performance metrics of ME materials in different applications.

Table 2 Characterization of different applications

Areas of application	Lower limit of detection (LOD)	Operating bandwidth	magnetoelectric sensitivities
MAD Applications[64]	0.03nT	0.1~100Hz	88.4V/Oe
DC Magnetic Field Detection[15]	0.8nT	DC	14.9 V/Oe
Nondestructive Testing[67]	/	121kHz	/
Magnetoelectric Compass[68]	1000nT	0~50Hz	0.036 V/cm·Oe
Biosensors[69]	0.02nT	10~15kHz	930 V/Oe
Communications Antenna[75]	0.47nT	0-1kHz	/

The following section IV.A-G will expand on each type of application.

A. MAD Applications

Magnetic anomaly detection (MAD) is a detection method that utilizes the anomalous geomagnetic signals produced by magnetic objects within the geomagnetic field for identification. It has been extensively employed in engineering and environmental geophysical exploration and has emerged as a prevalent approach for implementing magnetic field sensors in contemporary times. Currently, the magnetic anomaly detection and positioning technology is developing rapidly. By building a three-axis sensor system and combining it with positioning algorithms, multi-scenario applications can be realized. For example, Ziyun Chen from Shanghai Jiaotong University led a team to independently design a triaxial ME sensor [64]. Each single axis of the sensor consists of a MNdoped PMN-PT/Metglas core sensitive element. A low-noise pre-charge amplifier circuit and a three-axis sensor test system were constructed.

In addition, a hybrid algorithm consisting of the particle swarm optimization algorithm and an annealing algorithm combined with the abovementioned three-axis sensors is proposed. The goodness indices of each axis sensor in the experimental tests reach high values of 0.9182, 0.9287, and 0.9320. It is highly reliable and accurate in estimating the kinematic parameters of the ferromagnetic target in MAD.

Similarly, Ying Shen et al. from Virginia Tech proposed a vehicle detection method based on a three-axis ME sensor [16]. The core sensitive element consists of three layers:

Metglas/Pb(Zr,Ti)O₃/Metglas, as shown in Fig. 9. On this basis, a 3D simulation model was developed to enable the localization and tracking of vehicles. The model is nonintrusive, is low-cost, has low power consumption, and is portable.

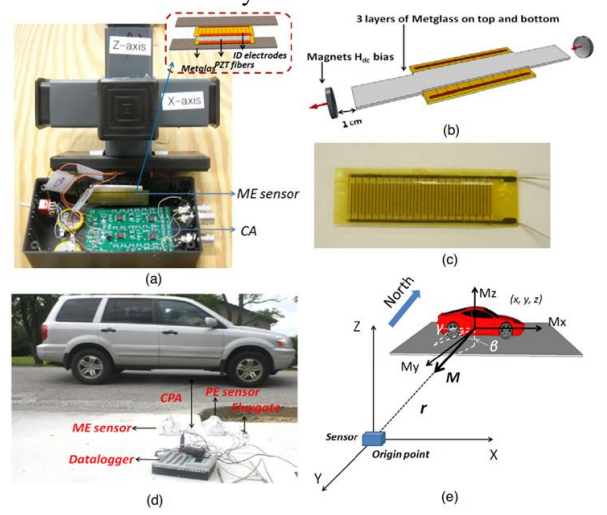


Fig. 9 (a) Photograph of the prototype triple-layer ME sensor detection unit composed of an ME sensor and a charge amplifier. The inset shows the configuration of the Metglas/PZT/Metglas ME laminates. (b) Schematic of the ME sensor. (c) Photograph of the PE sensor. (d) Photograph of the vehicle detection system setup. (e) Three-dimensional components of the vehicle-induced magnetic fields [16].

B. DC Magnetic Field Detection

ME sensors have the advantages of low cost and high sensitivity and have great potential in the field of magnetic field detection. However, because their operation is based on the ME coupling effect, ME sensors cannot measure DC magnetic fields directly. To address this problem, Chu et al. combined a magnetoelectric composite with a fluxgate sensor structure [65]. and proposed a magnetoelectric fluxgate sensor for weak DC magnetic field detection. As shown in Fig 10, this sensor adopts a shuttle structure. The sensor uses Metglas as the magnetic core and magnetostrictive core to generate closed-loop high-frequency magnetic flux and longitudinal vibration. A pair of embedded piezoelectric PMN-PT fibers act as ME flux gates to detect magnetic anomalies in

differential mode. The sensors provide a 4- to 5-fold increase in output signal compared to past magneto-electric sensors at an applied DC magnetic signal of 1 nT.

In addition, an ME sensor based on a pair of highly coherent Metglas/Mn-PMNT/Metglas was proposed by Chen Rui et al. at the University of Chinese Academy of Sciences. The sensor consists of a pair of ME sensors modulated by 180° by reversing the AC magnetic field and an intelligent differential configuration of the ME sensors [15]. This sensor achieves a low detection limit of 0.8 nT for DC magnetic fields with a sensitivity of up to 14.9 V/Oe. This finding further opens up the application of ME sensors for DC magnetic field detection.

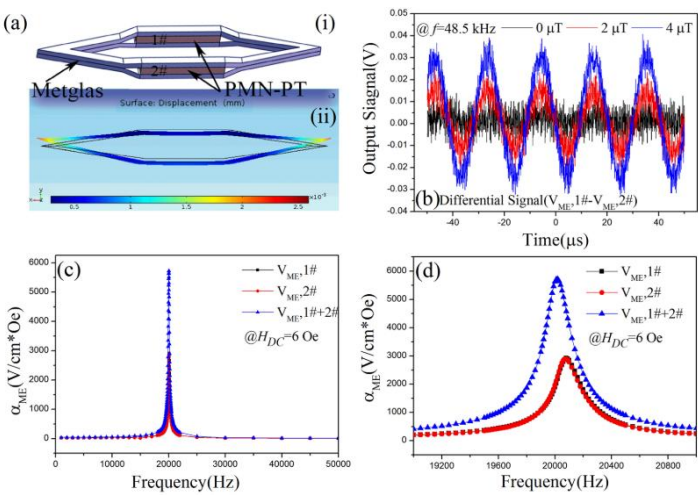


Fig 10 The experimental verification concerning the working principle and the ME performance for our proposed ME Gate sensor[65]: (a) Three-dimensional view of the ME flu gate sensor and a schematic view of the forced vibration mode at non resonant frequency.(b, c) The differential signal output of the MEFGS in response to varying DC magnetic field. (d) The sum ME signal output of two halves.

C. Nondestructive Testing

Nondestructive testing (NDT) is an indispensable technology for industrial development. Magnetic field signals are widely used for NDT of mechanical materials, such as in mechanical troubleshooting and pipeline condition detection. Compared with other non-destructive testing methods, magnetic non-destructive testing can realize non-contact and online real-time inspection.

According to the method of magnetic field signal formation, it can be divided into active field testing (AFT) and passive field testing (PFT) [66]. AFT identifies defects by detecting the magnetized magnetic field of the object under test, while PFT identifies defects only by detecting the external magnetic field of the material. With the improvement of the measurement accuracy of magnetic field sensors, PFT has become a hot research topic in NDT. The excellent performance of ME sensors makes them have a good application prospect in the field of PFT.

Recently, Jianglei Chang et al. from Shenzhen University first proposed a dual-mechanism integrated hybrid transducer and multimodal system based on ME effect measurements (ME-ACFM) and dual piezoelectric ultrasonic detection (DP-UT) in an alternating current (AC) field [67]. The system consists of a three-layer Metglas/PMN-PT/Metglas composite ME transducer wrapped by a coil and a dual piezoelectric ceramic ultrasound transducer, as shown in Fig 11. The hybrid transducer in the system detects both external and internal damage.

This technique provides important insights for future transducer designs based on multiphysics mechanisms. Enhanced quantitative characterization of large surface defects could also focus future research on more in-depth data fusion, multifrequency hybrid transducer and array design, and 3D b-field acquisition.

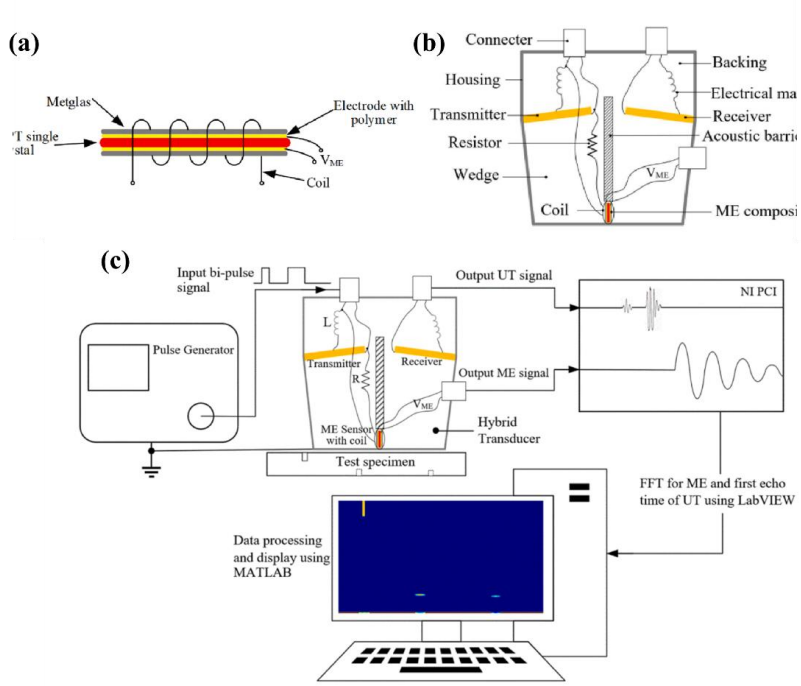


Fig 11 Schematic diagram of an ME ultrasound multimodal system for simultaneous nondestructive testing of a metal surface and internal defects [67]: (a) ME sensor with a coil. (b) Structure diagram of the hybrid transducer. (c) Block diagram of the workflow.

D. Magnetoelectric Compass

The magneto-electric compass is the key component that makes up the angle sensor. Angle sensors are widely used in various fields such as machinery, vehicles, aviation and navigation. Previously, angle sensors based on Hall effect, Giant Magnetoresistance, Anisotropic Magnetoresistance and Tunneling Magnetoresistance have been studied a lot [68]. ME sensors have a special advantage in the research of angle sensors by integrating the three physical fields of magneto-electricity. Based on ME materials, a magneto-electric compass was developed by Wu Jingen et al. It simultaneously detects the strength and direction of an AC magnetic field at

the surface [14]. This ME compass adopts a barbell-shaped structure as shown in Fig 12 and has excellent performance in detecting the in-plane AC magnetic field in any direction, in which the sensitivities of the magnetic field strength and angle are 0.01 Oe and $\pm 0.2^{\circ}$, respectively. In addition, this compass has the advantages of a simple structure, stable performance, and durability. The results of this research show that the ME compass in the angle sensor and compass has broad application prospects in marine navigation, vehicle navigation, industrial magnetic calibration, aircraft heading, magnetic detection, magnetic induction of power systems, among other areas.

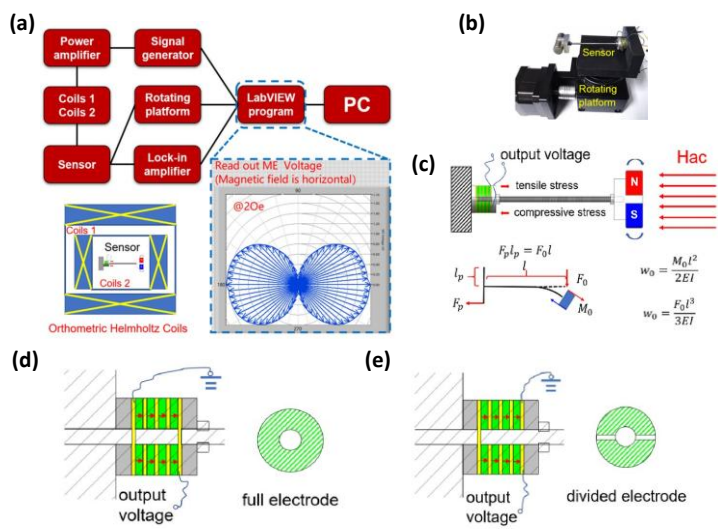


Fig 12 Magnetic compass for in-plane AC magnetic field detection [14]: (a) Experimental setup of the proposed ME compass. (b) Picture of the proposed sensor fixed on a rotating platform. (c) Schematic structure diagram of the proposed ME compass, as well as its mechanical analysis. (d) Schematic of the full electrode structure. (e) Schematic of the divided electrode structure.

E. Biosensors

Biomagnetic field detection can complement bioelectrical signal detection. Taking advantage of thin-film ME sensors, in recent years, Eric Elzenheimer et al. at the University of Kiel, Germany, designed an ME sensor system magnetocardiographic detection [69]. For the first time, they used an inverted ME thin-film sensor to detect human R-wave magnetic field equivalents in healthy volunteers. The system was successful in obtaining values in less than a minute, significantly reducing the time needed. The noise amplitude density of the system was less than 20 pT/Hz1/2 @10 Hz. For practical applications, the current sensor system is not sufficient for magnetic field detection of P- and T-waves. The signal-to-noise ratio at the output of the system needs to be

optimized to extract the cardiac signal more efficiently.

In addition, the research group at Kiel University has introduced a combined multi-scale 3D finite element method (FEM) model [70], as shown in Fig 13. The ME sensor array was combined with a human head model from MRI. This approach was used for brain bioelectricity detection. Future excitation models could also develop the head geometry demonstrated in this work to include more tissue regions at higher resolution, as well as different biological or artificial excitation sources. Examples include implanted DBS electrodes, leading to potential localization and orientation studies using patient- or application-specific head and ME sensor models.

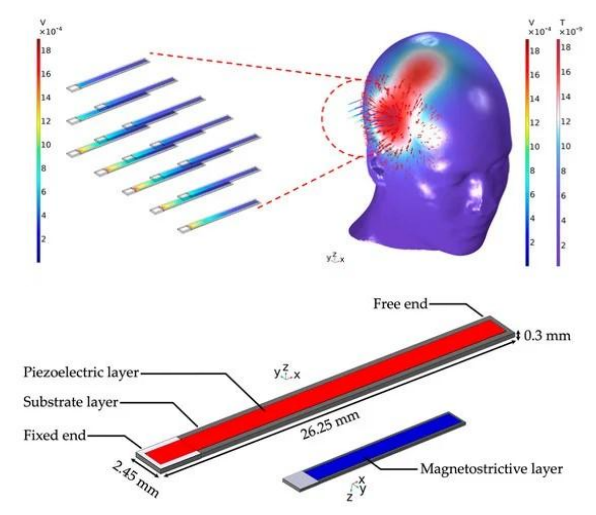


Fig 13 (a) The magnetic flux density norm on the head's surface with corresponding vector arrows and, based on this propagating magnetic field as the method of excitation, the electric response of an adjacent ME sensor array with 15 sensors. (b) The ME sensor model [70].

F. Energy Harvesters

The magnetic energy wasted in the environment can be captured via ME materials. Harvesting magnetic noise energy for utilization creates broader prospects for the application of magnetic field sensors. ME energy harvesters that

simultaneously harvest magnetic and vibrational energy were first proposed by Dong et al. in 2008 [71]. The energy harvesters operate on the basis of the magnetic moment effect. A change in the magnetic field deforms and vibrates the cantilevered beam, and the piezoelectric material senses the deformed mechanical energy and converts it into electrical

energy. Owing to the two-mechanism phenomenon, energy harvesters can obtain energy from both magnetic fields and mechanical vibrations.

Kambale et al. [13] made great strides in ME energy harvesters. Dong collaborated with Ryu et al. to prepare asymmetric and symmetric ME laminate structures of piezoelectric microfiber composites (MFCs)/nickel (Ni). The MFC/Ni ME energy harvester has self-bias characteristics. This provides future feasibility for designing magnetic field sensors and for powering small consumer electronics devices and wireless sensor network systems by utilizing surrounding mechanical/magnetic stimulation. The energy harvester developed by Dong et al. subsequently achieved a maximum power density of 11.73 μW/Oe²cm³ at short and open resonant

frequencies (<100 Hz) [12]. This value is an order of magnitude greater than the maximum power density of previously reported ME energy harvesters.

In 2020, the research team of Zhonghui Yu and Zhaoqiang Chu et al. developed a rectangular cymbal-shaped energy harvester consisting of PZT piezoelectric ceramics and a Metglas magnetostrictive material, which further improved the MME energy harvester [72]. Its structure is shown in Fig. 14(a). The power density was 5.1 mV/cm³ under a 7 Oe AC magnetic field. Compared with the previous performance of MME energy harvesters, which are composed of piezoelectric single crystals, this device had better piezoelectric performance.

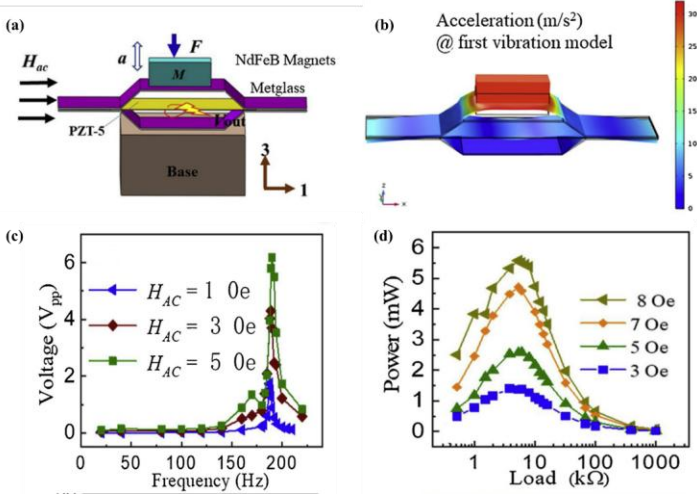


Fig. 14 (a) Schematic diagram and structure of the MME energy harvester. (b) FEA modelling results of the rectangular cymbal structure under AC magnetic field excitation, H_{AC} -induced acceleration, and deformation in the first vibration model. (c) Open-circuit peak-peak output voltage under varying H_{AC} . (d) Generated power of the MME energy harvester as a function of the load resistance under varying H_{AC} excitations [72].

In 2023, Zhonghui Yu's research team published another magneto-mechanical-electrical coupled energy harvester (MMEC-EH) based on the piezoelectric ceramic PMNN-PZT in the journal AFM [73]. Using the cantilever beam structure, under the action of an AC magnetic field or an external force, the stress concentration effect of the cantilever will occur at the narrow end of the connected piezoelectric ceramic sheet. Its structure and force are shown in Fig 15(a). Under the double excitation of an AC magnetic field of $H_{\rm AC}=0.5$ Oe, the vibration acceleration was a=0.05 g. As shown in Fig

15(c, d), two excitation signals are summed to calculate the total output power density, and the corresponding RMS power density in the PMNN-PZT MMEC-EH is 60 mW_{RMS}Oe⁻²g⁻² cm⁻³. This performance is double the previously developed piezoelectric ceramic MMEC-EH. In addition, this study successfully applied energy harvesters to power temperature/humidity sensors, demonstrating the feasibility of harvesting vibration and magnetic field energy from the environment and applying it to self-supplied ME sensors.

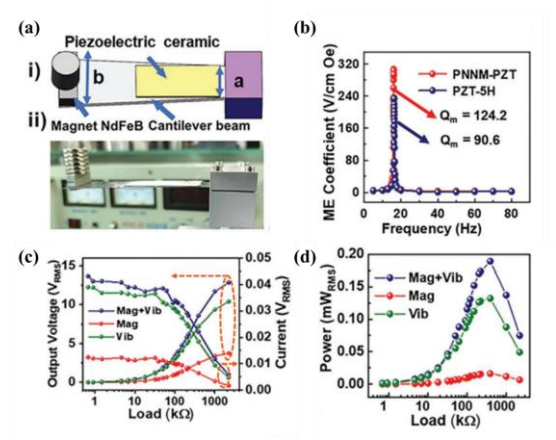


Fig 15 (a) i) ii) Schematic and photo of the designed MMEC-EHs with the cantilever structure. (b) i) FEA result for deformation of the MMEC-EH in its first-

order bending vibration mode, ii) MMEC-EH energy harvester operating principle equivalent circuit diagrams. (c)(d) Output RMS voltage, current, and power as a function of the external load resistance under different stimulation sources at resonance frequency [73].

G. Communications Antenna

The enhanced performance of ME sensors at resonant frequencies gives them the potential to far surpass all current types of sensors in terms of mechanical antennas. A team of SUN et al. at Northeastern University in Boston, Massachusetts, USA, developed an ultracompact, dual-frequency, smart nanoelectromechanical system ME antenna for use in ultracompact wireless implantable medical devices [74]. The antenna measures only $250 \times 174 \ \mu m^2$ and consists of three parallel rectangular ME resonators, each measuring $250 \times 50 \ \mu m^2$, as shown in Fig. 16(a). It is capable of efficiently performing wireless energy harvesting and sensing ultrasmall magnetic fields at the level of neuromagnetic fields.

This dual-frequency ME antenna has two acoustic resonance frequencies: 2.51 GHz and 63.6 MHz. The former is used for wireless RF energy harvesting, and the latter is used for low-frequency magnetic field sensing, which can be used for neural recordings. The improved power transfer efficiency allows implantable devices to operate deeper in the body, which has promising applications in the biomedical field.

In addition, SUN et al. designed a novel very low-frequency (VLF) communication system based on a pair of ME antennas [75], as shown in Fig. 16(c). The system works at a VLF electromechanical resonance frequency, and the measured communication distance can reach 120 m. However, the simulation results show that the system can achieve a

transmission distance of approximately 10 km under the conditions of enhanced radiation intensity and with an optimized receiver. This means that this communication system has great long-distance transmission potential.

Antenna miniaturization technology is also the research hotspot of ME antennas at present, and many research teams have made remarkable achievements in this area. Considering the limitations of the principle of electromagnetic radiation on the miniaturization of ME antennas, Xiangyang Li and his team at Xidian University have made a new attempt. They reduced the structural size of the antenna by nearly two orders of magnitude by using acoustic excitation instead of electromagnetic radiation [76], as shown in Fig. 16(e). An antenna sample with a working frequency of 2.45 GHz and gain of 15.59 dB is successfully prepared, which provides a new scheme for antenna miniaturization. The team of Professor Zhibo Ma and others from Northwestern Polytechnical University applied MEMS ME materials to the development of ME antennas [77], as shown in Fig. 16(g). They conducted miniaturization research on the antenna by reducing the volume of sensitive components. The experimental tests proved that when the mechanical resonant frequency of the MEMS ME antenna was 224.1 kHz, the ME coupling coefficient was 2.928 kV/cm/Oe. It is sensitive to specific frequency electromagnetic waves and has the potential to become an ultrasensitive magnetic sensor.

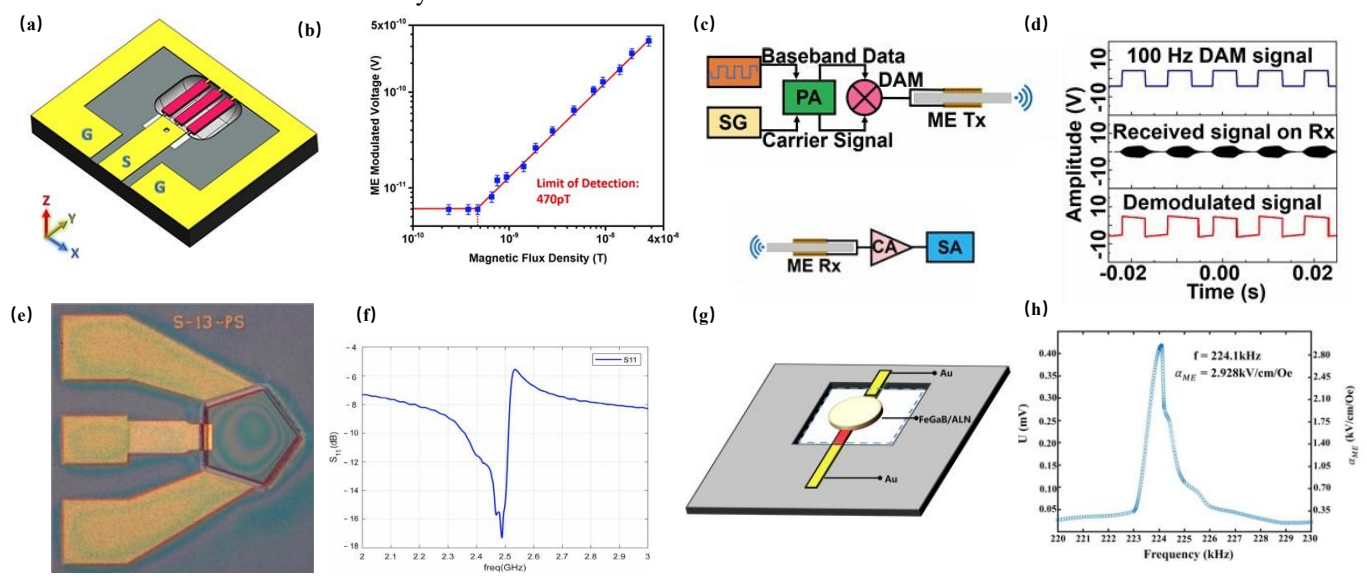


Fig. 16 (a) 3D schematic of the ME antenna on a released Si substrate. The yellow colour indicates a gold ground ring and GSG pads that are used for probing and wire bonding the antenna to the PCB. (b) ME-modulated voltage versus the amplitude of the external magnetic field Hm at a frequency of 1 kHz, showing an LOD of 470 pT [74]. (c) Schematic of the communication link between the ME Tx and Rx; in the blocks, SG, PA, CA, and SA stand for the signal generator, power amplifier, charge amplifier, and spectrum analyser, respectively. (d) From top to bottom: 100 Hz bit stream modulated on ME Tx, the signal received by ME Rx, and the 100 Hz bit stream recovered after demodulation [75]. (e) Optical image of the ME antenna. (f) Reflection coefficient (S11) curve of the ME antenna [76]. (g) Structural dimensions of the developed MEMS ME antenna. (h) MEMS ME antenna output signal and ME coefficient [77].

V. FUTURE PROSPECTIVE

This review provides a comprehensive overview of the evolution of various types of ME materials. More importantly, the latest research works about the applications of ME devices have been summarized, such as biosensors, flexible sensors

and communication antennas. Hopefully, it can provide more prospective idea about the development of ME devices in future. However, there are still several pressing issues that have not been resolved; therefore, there is much room for improvement. In terms of material development, the current research on multiferroics is not comprehensive enough. The

exploration of ferromagnetic and ferroelectric multiferroics with better performance is extremely urgent. On the basis of better materials, the development of magnetoelectrically coupled materials may have broader prospects. In addition, different coupling mechanisms directly affect the ME coefficients and application areas of ME-coupled materials. Improving the mechanical conduction efficiency between the phases of materials and optimizing the coupling mechanism remain key focuses of R&D work. Finally, miniaturized products offer greater advantages in practical applications. Reducing the size of ME materials to achieve miniature ME sensors with high sensitivity is also an important optimization direction.

At present, compared with mature sensors on the market, ME sensors are still in the experimental stage. There is a gap in the actual performance, and there are many urgent problems to be solved in terms of application, such as the environmental adaptability problem, signal processing problems, and the problem of detecting engineering deployment. Therefore, to broaden the potential application areas of sensors, the current key is to solve the problem of sensor packaging and its signal processing circuit design. In addition, there is a need to implement industry-specific production standards to achieve greater industrialization and promote more applications.

VI. REFERENCES

- [1] C. W. Nan, Y. Lin, and J. H. Huang, "Magnetoelectricity of Multiferroic Composites," *Ferroelectrics*, vol. 280, no. 1, pp. 153-163, 2011.
- [2] M. Fiebig, "Revival of the magnetoelectric effect," *Journal of Physics D: Applied Physics*, vol. 38, no. 8, pp. R123-R152, 2005.
- [3] W. Prellier, M. P. Singh, and P. Murugavel, "The single-phase multiferroic oxides: from bulk to thin film," *Journal of Physics: Condensed Matter*, vol. 17, no. 30, pp. R803-R832, 2005.
- [4] Y. Tokura and S. Seki, "Multiferroics with Spiral Spin Orders," *Advanced Materials*, vol. 22, no. 14, pp. 1554-1565, 2010.
- [5] M. M. SANG-WOOK CHEONG, "Multiferroics: a magnetic twist for ferroelectricity," *nature materials*, vol. 6, pp. 13-20, 2007.
- [6] S. Priya, R. Islam, S. Dong, and D. Viehland, "Recent advancements in magnetoelectric particulate and laminate composites," *Journal of Electroceramics*, vol. 19, no. 1, pp. 149-166, 2007.
- [7] J. Ryu, S. Priya, K. Uchino, and H.-E. Kim, "Magnetoelectric Effect in Composites of Magnetostrictive and Piezoelectric Materials," Journal of Electroceramics, vol. 8, pp. 107–119, 2002
- [8] J. Ryu, S. Priya, K. Uchino, H.-E. Kim, and D. Viehland, "High Magnetoelectric Properties in 0.68Pb(Mg1/3Nb2/3)O3-0.32PbTiO3 Single Crystal and Terfenol-D Laminate Composites," *Journal of the Korean Ceramic Society*, vol. 39, no. 9, pp. 813-817, 2002.
- [9] Z. Chu et al., "Enhanced Resonance Magnetoelectric

- Coupling in (1-1) Connectivity Composites," *Advanced Materials*, vol. 29, no. 19, p. 1606022, 2017.
- [10] Z. Chu, M. PourhosseiniAsl, and S. Dong, "Review of multi-layered magnetoelectric composite materials and devices applications," *Journal of Physics D: Applied Physics*, vol. 51, no. 24, p. 243001, 2018.
- [11] X. Zhuang *et al.*, "Analysis of Noise in Magnetoelectric Thin-Layer Composites Used as Magnetic Sensors," *IEEE Sensors Journal*, vol. 11, no. 10, pp. 2183-2188, 2011.
- [12] G. Liu, P. Ci, and S. Dong, "Energy harvesting from ambient low-frequency magnetic field using magneto-mechano-electric composite cantilever," *Applied Physics Letters*, vol. 104, no. 3, p. 032908, 2014.
- [13] R. C. Kambale *et al.*, "Magneto-Mechano-Electric (MME) Energy Harvesting Properties of Piezoelectric Macro-fiber Composite/Ni Magnetoelectric Generator," *Energy Harvesting and Systems*, vol. 1, no. 1-2, pp. 3-11, 2014.
- [14] J. Wu et al., "A Magnetoelectric Compass for In-Plane AC Magnetic Field Detection," *IEEE Transactions on Industrial Electronics*, vol. 68, no. 4, pp. 3527-3536, 2021.
- [15] R. Chen *et al.*, "Differential Configuration for Highly Sensitive DC Magnetic Field Sensing Based on Nonlinear Magnetoelectric Effect," *IEEE Sensors Journal*, vol. 22, no. 18, pp. 17754-17760, 2022.
- [16] J. Gao, D. Hasanyan, Y. Shen, Y. Wang, J. Li, and D. Viehland, "Giant resonant magnetoelectric effect in bi-layered Metglas/Pb(Zr,Ti)O3 composites," *Journal of Applied Physics*, vol. 112, no. 10, p. 104101, 2012.
- [17] P. Curie, "On Symmetry in Physical Phenomena," *Journal de Physique*, vol. 3, no. 3, pp. 393-415, Sep. 1894.
- [18] P. Debye, "Remark to some new trials on a magnetoelectrical direct effect," *ZEITSCHRIFT FUR PHYSIK*, vol. 36, pp. 300-301, 1926.
- [19] V. J. Folen, G. T. Rado, and E. W. Stalder, "Anisotropy of the Magnetoelectric Effect inCr2O3," *Physical Review Letters*, vol. 6, no. 11, pp. 607-608, 1961.
- [20] J. v. Suchtelen, "Product Properties: A new application of composite materials," *Philips Research Reports*, vol. 27, no. 1, pp. 28-37, 1972.
- [21] C.-W. Nan, M. I. Bichurin, S. Dong, D. Viehland, and G. Srinivasan, "Multiferroic magnetoelectric composites: Historical perspective, status, and future directions," *Journal of Applied Physics*, vol. 103, no. 3, p. 031101, 2008.
- [22] J. Boomgaard, D. Terrell, R. Born, and H. Giller, "An In-Situ Grown Eutectic Magnetoelectric Composite Material, Part 1: Composition and Unidirectional Solidification[J].Journal of Materials Science," *Journal of Materials Science*, vol. 9, no. 10, pp. 1705-1709, 1974.
- [23] J. Ryu, A. V. a. CARAZO, K. UCHINO, and H.-E. KIM, "Magnetoelectric Properties in Piezoelectric and Magnetostrictive Laminate Composites," *Jpn. J.*

- Appl. Phys, vol. 40, no. 8, pp. 4948-4951, 2001.
- [24] G. Srinivasan, E. T. Rasmussen, J. Gallegos, R. Srinivasan, Y. I. Bokhan, and V. M. Laletin, "Magnetoelectric bilayer and multilayer structures of magnetostrictive and piezoelectric oxides," *Physical Review B*, vol. 64, no. 21, p. 214408, 2001.
- [25] J. Zhai, S. Dong, Z. Xing, J. Li, and D. Viehland, "Giant magnetoelectric effect in Metglas/polyvinylidene-fluoride laminates," *Applied Physics Letters*, vol. 89, no. 8, p. 083507, 2006.
- [26] S. Dong, J. Zhai, J. Li, and D. Viehland, "Near-ideal magnetoelectricity in high-permeability magnetostrictive/piezofiber laminates with a (2-1) connectivity," *Applied Physics Letters*, vol. 89, no. 25, p. 252904, 2006.
- [27] J. Ma, Z. Shi, and C. W. Nan, "Magnetoelectric Properties of Composites of Single Pb(Zr,Ti)O3 Rods and Terfenol-D/Epoxy with a Single-Period of 1-3-Type Structure," *Advanced Materials*, vol. 19, no. 18, pp. 2571-2573, 2007.
- [28] M. Li et al., "Enhanced Sensitivity and Reduced Noise Floor in Magnetoelectric Laminate Sensors by an Improved Lamination Process," Journal of the American Ceramic Society, vol. 94, no. 11, pp. 3738-3741, 2011.
- [29] J. Gao, L. Shen, Y. Wang, D. Gray, J. Li, and D. Viehland, "Enhanced sensitivity to direct current magnetic field changes in Metglas/Pb(Mg1/3Nb2/3)O3–PbTiO3 laminates," *Journal of Applied Physics*, vol. 109, no. 7, p. 074507, 2011.
- [30] G. Sreenivasulu, L. Y. Fetisov, Y. K. Fetisov, and G. Srinivasan, "Piezoelectric single crystal languatate and ferromagnetic composites: Studies on low-frequency and resonance magnetoelectric effects," *Applied Physics Letters*, vol. 100, no. 5, p. 052901, 2012.
- [31] C. Kirchhof *et al.*, "Giant magnetoelectric effect in vacuum," *Applied Physics Letters*, vol. 102, no. 23, p. 232905, 2013.
- [32] E. Yarar *et al.*, "Inverse bilayer magnetoelectric thin film sensor," *Applied Physics Letters*, vol. 109, no. 2, p. 022901, 2016.
- [33] A. V. Turutin *et al.*, "Magnetoelectric metglas/bidomain y + 140°-cut lithium niobate composite for sensing fT magnetic fields," *Applied Physics Letters*, vol. 112, no. 26, p. 262906, 2018.
- [34] M. PourhosseiniAsl *et al.*, "Versatile power and energy conversion of magnetoelectric composite materials with high efficiency via electromechanical resonance," *Nano Energy*, vol. 70, p. 104506, 2020.
- [35] J. Lou, G. N. Pellegrini, M. Liu, N. D. Mathur, and N. X. Sun, "Equivalence of direct and converse magnetoelectric coefficients in strain-coupled two-phase systems," *Applied Physics Letters*, vol. 100, no. 10, p. 102907, 2012.
- [36] Y. Cheng, B. Peng, Z. Hu, Z. Zhou, and M. Liu, "Recent development and status of magnetoelectric materials and devices," *Physics Letters A*, vol. 382, no. 41, pp. 3018-3025, 2018.
- [37] Q. Zhang et al., "Enhanced piezoelectric and

- ferroelectric properties in Mn-doped Na0.5Bi0.5TiO3–BaTiO3 single crystals," *Applied Physics Letters*, vol. 95, no. 10, p. 102904, 2009.
- [38] T. Deng *et al.*, "Significant improving magnetoelectric sensors performance based on optimized magnetoelectric composites via heat treatment," *Smart Materials and Structures*, vol. 30, no. 8, p. 085005, 2021.
- [39] F. Wang, L. Luo, D. Zhou, X. Zhao, and H. Luo, "Complete set of elastic, dielectric, and piezoelectric constants of orthorhombic 0.71Pb(Mg1/3Nb2/3)O3–0.29PbTiO3 single crystal," *Applied Physics Letters*, vol. 90, no. 21, p. 212903, 2007.
- [40] J. Gao, J. Das, Z. Xing, J. Li, and D. Viehland, "Comparison of noise floor and sensitivity for different magnetoelectric laminates," *Journal of Applied Physics*, vol. 108, no. 8, p. 084509, 2010.
- [41] S. Dong, J.-F. Li, and D. Viehland, "Characterization of magnetoelectric laminate composites operated in longitudinal-transverse and transverse—transverse modes," *Journal of Applied Physics*, vol. 95, no. 5, pp. 2625-2630, 2004.
- [42] S. Dong and J. Zhai, "Equivalent circuit method for static and dynamic analysis of magnetoelectric laminated composites," *Science Bulletin*, vol. 53, no. 14, pp. 2113-2123, 2008.
- [43] F. Fang, C. Zhao, and W. Yang, "Thickness effects on magnetoelectric coupling for Metglas/PZT/Metglas laminates," *Science China Physics, Mechanics and Astronomy*, vol. 54, no. 4, pp. 581-585, 2011.
- [44] V. M. P. M.I. Bichurin, "Theory of Low Frequency Magnetoelectric Coupling in Magnetostrictive Piezoelectric Bilayers," *Physical Review B*, vol. 68, no. 5, p. 054402, 2003.
- [45] M. Li, D. Hasanyan, Y. Wang, J. Gao, J. Li, and D. Viehland, "Theoretical modelling of magnetoelectric effects in multi-push-pull mode Metglas/piezo-fibre laminates," *Journal of Physics D: Applied Physics*, vol. 45, no. 35, p. 355002, 2012.
- [46] D. Hasanyan *et al.*, "Theoretical and experimental investigation of magnetoelectric effect for bendingtension coupled modes in magnetostrictive-piezoelectric layered composites," *Journal of Applied Physics*, vol. 112, no. 1, p. 013908, 2012.
- [47] Y. Wang *et al.*, "Influence of interfacial bonding condition on magnetoelectric properties in piezofiber/Metglas heterostructures," *Journal of Alloys and Compounds*, vol. 513, pp. 242-244, 2012.
- [48] S. Dong, J. Cheng, J. F. Li, and D. Viehland, "Enhanced magnetoelectric effects in laminate composites of Terfenol-D/Pb(Zr,Ti)O3 under resonant drive," *Applied Physics Letters*, vol. 83, no. 23, pp. 4812-4814, 2003.
- [49] S. Dong, J.-F. Li, and D. Viehland, "Longitudinal and Transverse Magnetoelectric Voltage Coefficients of Magnetostrictive/Piezoelectric Laminate Composite: Theory," *IEEE Transactions on Ultrasonics, Ferroelectrics, and Frequency Control,* vol. 50, no. 10, pp. 1253-1261, 2003.
- [50] S. Dong, J. Zhai, F. Bai, J.-F. Li, and D. Viehland,

- "Push-pull mode magnetostrictive/piezoelectric laminate composite with an enhanced magnetoelectric voltage coefficient," *Applied Physics Letters*, vol. 87, no. 6, p. 062502, 2005.
- [51] J. Zhang *et al.*, "Bidirectional tunable ferritepiezoelectric trilayer magnetoelectric inductors," *Applied Physics Letters*, vol. 113, no. 11, p. 113502, 2018.
- [52] M. I. Bichurin *et al.*, "Self-Biased Bidomain LiNbO3/Ni/Metglas Magnetoelectric Current Sensor," *Sensors*, vol. 20, no. 24, p. 7142, 2020.
- [53] D. Rajaram Patil *et al.*, "Enhancement of resonant and non-resonant magnetoelectric coupling in multiferroic laminates with anisotropic piezoelectric properties," *Applied Physics Letters*, vol. 102, no. 6, p. 062909, 2013.
- [54] Y. Wang *et al.*, "An Extremely Low Equivalent Magnetic Noise Magnetoelectric Sensor," *Advanced Materials*, vol. 23, no. 35, pp. 4111-4114, 2011.
- [55] J. gao *et al.*, "Differential-Mode Vibrational Noise Cancellation Structure for Metglas/Pb(Zr,Ti)O3 Fiber Magnetoelectric Laminates," *IEEE Transactions on Ultrasonics, Ferroelectrics, and Frequency Control*, vol. 58, no. 8, pp. 1541-1544, 2011.
- [56] C. Fang et al., "Significant reduction of equivalent magnetic noise by in-plane series connection in magnetoelectric Metglas/Mn-doped Pb(Mg1/3Nb2/3)O3-PbTiO3 laminate composites," Journal of Physics D: Applied Physics, vol. 48, no. 46, p. 465002, Oct.20 2015.
- [57] N. Yang *et al.*, "Ultrasensitive flexible magnetoelectric sensor," *APL Materials*, vol. 9, no. 2, p. 021123, 2021.
- [58] L. W. Martin, Y. H. Chu, and R. Ramesh, "Advances in the growth and characterization of magnetic, ferroelectric, and multiferroic oxide thin films," *Materials Science and Engineering: R: Reports*, vol. 68, no. 4-6, pp. 89-133, 2010.
- [59] H. Greve, E. Woltermann, H.-J. Quenzer, B. Wagner, and E. Quandt, "Giant magnetoelectric coefficients in (Fe90Co10)78Si12B10-AlN thin film composites," *Applied Physics Letters*, vol. 96, no. 18, p. 182501, 2010.
- [60] P. Hayes *et al.*, "Electrically modulated magnetoelectric sensors," *Applied Physics Letters*, vol. 108, no. 18, p. 182902, 2016.
- [61] A. Kittmann *et al.*, "Wide Band Low Noise Love Wave Magnetic Field Sensor System," *Scientific Reports*, vol. 8, no. 1, p. 278, 2018.
- [62] T. Nan, Y. Hui, M. Rinaldi, and N. X. Sun, "Self-Biased 215MHz Magnetoelectric NEMS Resonator for Ultra-Sensitive DC Magnetic Field Detection," Scientific Reports, vol. 3, no. 1, p. 1985, 2013.
- [63] F. Huang *et al.*, "MEMS Surface Acoustic Wave Resonator Based on AlN/Si/Fe–Co–Si–B Structure for Magnetic Field Sensing," *IEEE Sensors Journal*, vol. 22, no. 23, pp. 22510-22518, 2022.
- [64] Z. Chen *et al.*, "Magnetic Anomaly Detection Using Three-Axis Magnetoelectric Sensors Based on the Hybridization of Particle Swarm Optimization and

- Simulated Annealing Algorithm," *IEEE Sensors Journal*, vol. 22, no. 4, pp. 3686-3694, 2022.
- [65] Z. Chu *et al.*, "A magnetoelectric flux gate: new approach for weak DC magnetic field detection," *Scientific Reports*, vol. 7, no. 1, p. 8592, 2017.
- [66] Z. D. Wangn, Y. Gu, and Y. S. Wang, "A review of three magnetic NDT technologies," *Journal of Magnetism and Magnetic Materials*, vol. 324, pp. 382–388, 2011.
- [67] J. Chang, Z. Chu, X. Gao, A. I. Soldatov, and S. Dong, "A magnetoelectric-ultrasonic multimodal system for synchronous NDE of surface and internal defects in metal," *Mechanical Systems and Signal Processing*, vol. 183, p. 109667, 2023.
- [68] A. S. A. Kumar, B. George, and S. C. Mukhopadhyay, "Technologies and Applications of Angle Sensors: A Review," *IEEE Sensors Journal*, vol. 21, no. 6, pp. 7195-7206, 2021.
- [69] E. Elzenheimer *et al.*, "Investigation of Converse Magnetoelectric Thin-Film Sensors for Magnetocardiography," *IEEE Sensors Journal*, vol. 23, no. 6, pp. 5660-5669, 2023.
- [70] M.-Ö. Özden, G. Barbieri, and M. Gerken, "A Combined Magnetoelectric Sensor Array and MRI-Based Human Head Model for Biomagnetic FEM Simulation and Sensor Crosstalk Analysis," *Sensors*, vol. 24, no. 4, p. 1186, 2024.
- [71] S. Dong, J. Zhai, J. F. Li, D. Viehland, and S. Priya, "Multimodal system for harvesting magnetic and mechanical energy," *Applied Physics Letters*, vol. 93, no. 10, p. 103511, 2008.
- [72] Z. Yu *et al.*, "A magneto-mechano-electric (MME) energy harvester based on rectangular cymbal structure," *Sensors and Actuators A: Physical*, vol. 316, p. 112400, 2020.
- [73] Z. Yu *et al.*, "A PMNN-PZT Piezoceramic Based Magneto-Mechano-Electric Coupled Energy Harvester," *Advanced Functional Materials*, vol. 32, no. 25, p. 2111140, 2022.
- [74] M. Zaeimbashi *et al.*, "Ultra-compact dual-band smart NEMS magnetoelectric antennas for simultaneous wireless energy harvesting and magnetic field sensing," *Nature Communications*, vol. 12, no. 1, p. 3141, 2021.
- [75] C. Dong *et al.*, "A Portable Very Low Frequency (VLF) Communication System Based on Acoustically Actuated Magnetoelectric Antennas," *IEEE Antennas and Wireless Propagation Letters*, vol. 19, no. 3, pp. 398-402, 2020.
- [76] N. Li, X. Li, B. Xu, B. Zheng, and P. Zhao, "Design and Optimization of a Micron-Scale Magnetoelectric Antenna Based on Acoustic Excitation," *Micromachines*, vol. 13, no. 10, p. 1584, 2022.
- [77] Y. Wang et al., "A Low-Frequency MEMS Magnetoelectric Antenna Based on Mechanical Resonance," Micromachines, vol. 13, no. 6, p. 864, 2022.